

Breakup dynamics and isotope effects in D_2H^+ and H_2D^+ dissociative recombinationD. Strasser,¹ L. Lammich,² H. Kreckel,² M. Lange,² S. Krohn,² D. Schwalm,² A. Wolf,² and D. Zajfman^{1,2}¹*Department of Particle Physics, Weizmann Institute of Science, Rehovot, 76100, Israel*²*Max-Planck-Institut für Kernphysik, D-69029 Heidelberg, Germany*

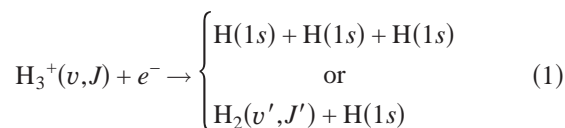
(Received 17 February 2004; published 15 June 2004)

The breakup dynamics of D_2H^+ and H_2D^+ following dissociative recombination with low energetic electrons has been studied combining two-dimensional imaging and storage ring techniques. The kinematical correlation between the hydrogen and deuterium atoms produced in the three-body channel was measured. We found that the three particles tend to dissociate with a geometry close to linear, and that the deuterium atom has a large probability to be at the center. The data also show that the remaining average internal excitation energy stored in the rotation of the D_2H^+ and H_2D^+ molecules corresponds to a temperature of less than 70 meV, much less than observed for the H_3^+ and D_3^+ species previously examined.

DOI: 10.1103/PhysRevA.69.064702

PACS number(s): 34.80.Lx

The triatomic hydrogen ion H_3^+ is the dominant positively charged molecular ion in all hydrogen containing plasma. Its destruction by dissociative recombination (DR) with free electrons, leading to neutral atomic and molecular fragments,



thus plays a key role in understanding the reaction dynamics and the atomic and molecular composition of these ionized systems. In particular, the DR rate coefficient and its influence on the abundance of H_3^+ and its isotopomers is a critical ingredient in astrochemical models of the cold interstellar medium [1], as these species play a dominant role in reactions which lead to molecule formation [2] and determine the deuteration fraction of interstellar molecules [3].

In view of its astrophysical importance and its benchmark character in quantum chemistry, the DR of cold H_3^+ ions and its isotopomers with low energetic electrons has been the subject of intensive experimental [4–6] and theoretical [7–9] studies during the last years. But despite these efforts and the apparent simplicity of the system, the DR process turned out to be a challenge to both experiment and theory. Experimentally, the control of the initial excitation of H_3^+ is the main issue, while theoretically the three dimensionality of the process constitutes the main difficulty. Complete energy dependences for the DR cross section have been measured at several storage rings [5,10–12] for H_3^+ , shown to be vibrationally but not rotationally relaxed prior to recombination [13], and rate coefficients of the order of $\alpha=1 \times 10^{-7} \text{ cm}^3 \text{ s}^{-1}$ for 300 K electrons have been deduced. In contrast, recent experiments using the flowing afterglow technique [14,15] have determined an upper limit of only $3 \times 10^{-9} \text{ cm}^3 \text{ s}^{-1}$ for the H_3^+ DR rate coefficient. While the difference between the two techniques remains unexplained, a calculation [8,9], which treats the fragmentation reaction in its full dimensionality, is supporting the storage ring results. Using storage rings, DR cross sections were measured also for the isotopomers of H_3^+ (Refs. [16–20]) and branching

ratios between the two- and three-body dissociation channel [see Eq. (1)] have been determined to be 1:3 for H_3^+ , D_3^+ , and H_2D^+ [18]; in addition, the $[HD]/2[H_2]$ ratio in the DR of H_2D^+ was found to be 1.20 ± 0.05 , slightly in favor of HD rather than H_2 production.

Recently, we have performed detailed experiments related to the dynamics of the breakup of H_3^+ and D_3^+ in the DR process [21–23] by measuring the kinematical correlation between the three hydrogen or deuterium atoms [see Eq. (1)]. It was found that the three neutral atoms produced by the DR reaction tend to dissociate along a straight line (while the original structure of the molecular ions is an equilateral triangle). An additional important outcome of these experiments has been the evidence for high ($kT_{\text{rot}} \sim 230 \text{ meV}$) rotational excitations of the molecular ions prior to recombination even after storage times of several tens of seconds. These results have led to storage ring experiments [5] and resulted in somewhat lower rate coefficients for H_3^+ when using an ion source producing rotationally colder ions.

In this work, we present an experimental study of the dissociation dynamics and of isotope effects in the DR of the isotopomers D_2H^+ and H_2D^+ , investigating the momentum distribution between the three neutral fragments. Our data also indicate that already after a short storage time the remaining rotational excitation for both D_2H^+ and H_2D^+ is considerably lower than observed for the symmetric species, an expected result as the asymmetric isotopomers, unlike H_3^+ and D_3^+ , have a nonvanishing permanent dipole moment (0.60 Debye and 0.48 Debye for H_2D^+ and D_2H^+ , respectively [24]) and can, therefore, radiatively cool both the vibrational and rotational motion.

The experiments were carried out at the Test Storage Ring (TSR) located at the Max-Planck-Institut für Kernphysik, Heidelberg, Germany applying a technique which has been previously described in detail [21]. In the present case, H_2D^+ (D_2H^+) ions were produced in a “hot” gas discharge ion source, and accelerated using a radio-frequency quadrupole accelerator to a kinetic energy of 1.9 meV for H_2D^+ and 1.2 meV for D_2H^+ before being injected into the storage ring. After each injection, about 10^6 ions were stored in the ring (55.4 m circumference) in an average vacuum of about

3×10^{-11} Torr, which ensured $1/e$ beam lifetimes of about 10 s. At each pass, the ion beam was merged over 1.5 m with a “cold” electron beam, which was produced by the TSR electron cooler and guided in the merging section by a magnetic field of 0.04 T. The electron beam had a 0.1 meV longitudinal and less than 25 meV transverse energy spread and was tuned such that the electrons and ions had the same average velocity. Thus, the average center-of-mass (CM) energy between the ions and electrons was approximately 10 meV.

In the interaction region, where the ion and electron beams are merged, neutral fragments are produced by the DR reaction. These fragments exit the ring and are detected using a two-dimensional (2D) imaging detector mounted straight ahead of the interaction region at a mean distance of 6 m. The 2D imaging detection scheme has been used extensively in the past years in several of our DR experiments, and details can be found in Ref. [21]. In the current detector setup, the 25 frames/s camera was replaced by a Dalsa CAD-6, 1000 frames/s digital camera, which was coupled to an image intensifier and a home-made frame grabber which can handle rates of up to 400 events/s. The imaging detector, which has a position resolution of $\sim 100 \mu\text{m}$, can resolve multiple hits which are separated on the surface of the detector by more than 1 mm; only events with three detected particles were included in the following analysis.

During the first few seconds of storage, which allows for the relaxation of the molecular ions, also the momentum spread of the ion beam is reduced by collisions with the cold electron beam, yielding very narrow beams with diameter of less than 1 mm (full width at half maximum). The shrinking of the beam size due to the phase space cooling by the electron cooler is essential for the data analysis, as the identification of the mass (H or D fragments) of the particle hitting the detector surface is made on the basis of their relative distance to the CM. For this purpose, all possible assignments are considered, and the combination with the calculated CM position being closest to the beam center is selected. Moreover, discrimination against random coincidence events is achieved by applying a cut on the CM distance from the beam center before the event is finally accepted. Monte Carlo simulations of the experiment show that for the H_2D^+ three-body dissociation channel, a 1σ cut on the CM distance from the beam center provides a correct identification in 93% of the accepted events (87% for D_2H^+), in agreement with estimates obtained from a more detailed analysis of the CM distance distribution (see below).

The kinetic energy release in the full fragmentation channel ($E_k=4.67$ eV for H_2D^+ and $E_k=4.72$ eV for D_2H^+) is distributed between the three atomic fragments. As the 2D imaging technique records distances in the detector plane, transverse to the beam velocity, only transverse velocities and energies can be measured. The transverse energy $E_{\perp i}$ of particle i is proportional to $A_i R_i^2$, where A_i is the mass number of the particle i (H or D), and R_i is the distance of particle i from the CM position measured on the surface of the imaging detector. In the same way $R^2 \equiv \sum_i A_i R_i^2$ is proportional to the total transverse kinetic energy release E_{\perp} . In Fig. 1, the probabilities $P(R^2)$, obtained by normalizing the measured R^2 distributions to unity (solid dots), are displayed at

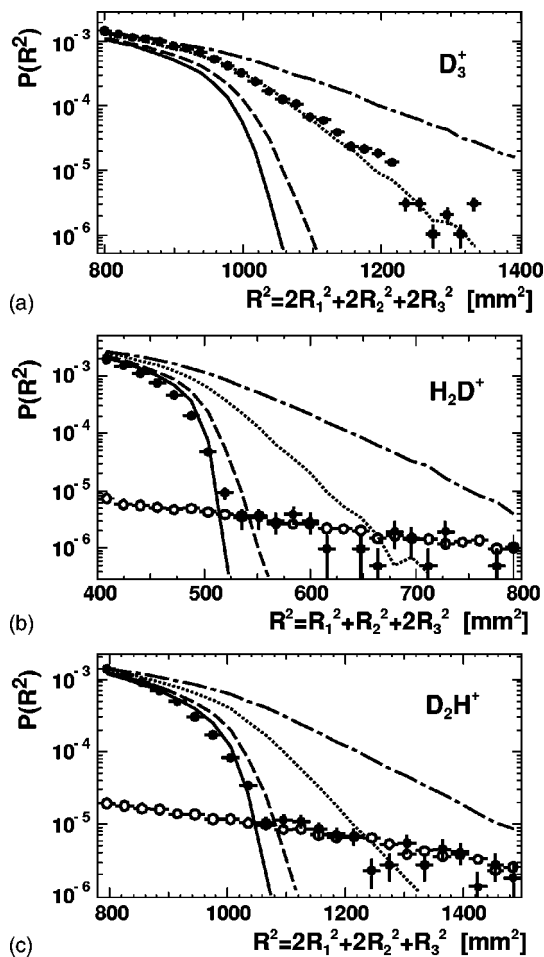


FIG. 1. Experimental R^2 distributions for three-fragment events following the DR of (a) D_3^+ , (b) H_2D^+ , and (c) D_2H^+ , recorded at storage time intervals of (a) 45–80 s, (b) 5–10 s, and (c) 10–60 s (solid dots). The open dots represent the background spectra due to misassigned events. The lines are the simulated R^2 spectra for rotationally cold molecular ions ($kT_{\text{rot}}=0$, solid lines), and for ions with rotational temperatures of $kT_{\text{rot}}=65$ meV (dashed lines), $kT_{\text{rot}}=230$ meV (dotted lines), and $kT_{\text{rot}}=500$ meV (dashed-dotted lines).

large values of R^2 for H_2D^+ (b) and D_2H^+ (c) and compared to the $P(R^2)$ distribution observed for D_3^+ (a) [23]. In contrast to the D_3^+ data, which are virtually background free, the flat tails of the measured $P(R^2)$ distributions at large R^2 values are due to misassigned events in the accepted event ensemble: The form and size of this contribution is well described by the corresponding background spectrum obtained by analyzing events far outside the CM distance cut. The solid lines represent the simulated distributions assuming rotationally cold molecular ions ($kT_{\text{rot}}=0$), while the dashed, dotted, and dashed-dotted lines correspond to simulations assuming spin-weighted Boltzmann distributions with characteristic rotational temperatures of $kT_{\text{rot}}=65$ meV, 230 meV, and 500 meV, respectively. Taking into account the systematic errors caused by the limited accuracy of the pixel to mm calibration of the camera as well as uncertainties due to the assumption of uncorrelated fragment momenta in the Monte Carlo simulations, an upper limit of kT_{rot}

≈ 70 meV can be deduced from the present experiment for the rotational temperature of H_2D^+ and D_2H^+ after 5 s of storage. This is also in good agreement with the data obtained by Lammich *et al.* [20] and the values given by Miller *et al.* [25] for highly excited rotational states. In contrast, D_3^+ (as well as H_3^+) display a rotational temperature of $kT_{\text{rot}} \approx 230$ meV even after 45 s of storage.

Due to energy and momentum conservation, the energy distribution between the three fragments determines uniquely the relative momenta of all fragments, including their relative directions in the dissociation plane. The dissociation geometry is defined in turn by a triangle, spanned by the velocity vectors of the three fragments in the comoving frame of reference of the molecular ion. The so-called ‘‘Dalitz plot’’ representation [26], which has already been used as a representation for the H_3^+ and D_3^+ three-body DR [21], is based on coordinates which are linear combinations of the energies of the dissociating particles. Representations in such coordinates have the advantage to produce a uniform distribution if the fragment momenta are uncorrelated (besides obeying total momentum conservation).

Since our 2D imaging system can only measure the transverse energies of the fragments, we choose to represent the measured transverse energy distribution by using ‘‘transversal’’ Dalitz coordinates [21], defined by linear combinations of the transverse energies $E_{\perp i}$ of the particles i . As the investigated systems are invariant under the exchange of two of the fragments, it is advantageous to define the transversal Dalitz coordinates, Q_1 and Q_2 , by

$$Q_1 = \frac{\sqrt{M/m_3}(E_{\perp 2} - E_{\perp 1})}{3E_{\perp}}, \quad (2)$$

$$Q_2 = \frac{(1 + m_3/m)E_{\perp 3} - E_{\perp 2} - E_{\perp 1}}{3E_{\perp}}, \quad (3)$$

where $m_1 = m_2 = m$ denotes the mass of the two identical particles, and E_{\perp} and M are defined as $E_{\perp} = E_{\perp 1} + E_{\perp 2} + E_{\perp 3}$, and $M = m_1 + m_2 + m_3$.

Each kinematically allowed coordinate pair (Q_1, Q_2) corresponds to a unique *projected* dissociation geometry; the shape of the triangles shown in the upper panels of Fig. 2 actually reflect for characteristic (Q_1, Q_2) values the hit pattern (modulo a rotation of each triangle around its center of mass) of the dissociation fragments as seen on the imaging detector for H_2D^+ [Fig. 2(a)] and D_2H^+ [Fig. 2(b)]. The allowed region in the (Q_1, Q_2) plane is limited to the inside of the circle of radius $\sqrt{Q_1^2 + Q_2^2} = 1/3$ by momentum conservation. The tangents to the circle shown by the solid lines are given by energy conservation and are obtained by setting the transverse energy of one of the particles to zero, e.g., the $Q_2 = -1/3$ line defines the points at which the odd atom received zero transverse energy, i.e., the D atom in H_2D^+ and the H atom in D_2H^+ . The symmetry of the two investigated systems obviously require a mirror symmetry around the $Q_1 = 0$ line.

It is easy to verify that the colinear *projected* dissociation geometries are located on the circumference and the triangular geometries in the middle of the circle. However, as the

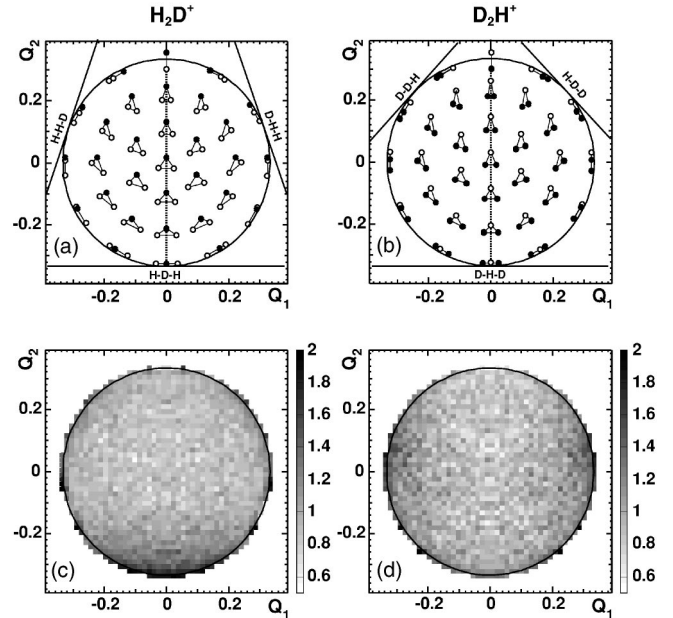


FIG. 2. (a) Kinematically allowed transversal Dalitz coordinates for H_2D^+ and projected dissociation geometries for a sample of points in the (Q_1, Q_2) plane. The dots show the position of the D, and the circles the position of the H. (b) Same as (a) but for D_2H^+ . (c) Weighted Dalitz plot for H_2D^+ . (d) Weighted Dalitz plot for D_2H^+ .

dissociation plane is randomly oriented with respect to the detector plane, there is no unique correspondence between the geometry in the dissociation plane and the projected geometry; each specific dissociation geometry is thus transformed into a variety of different projected geometries. For example, all the triangular geometries can be rotated such that their projections would be linear on the detector plane. This is why the number of events located on the circumference of the Q_1, Q_2 plot are enhanced relative to the number of counts observed at other projected dissociation geometries even when the 3 dim momenta of the fragmentation products are uncorrelated. In a previous paper [21], we have shown, that the most prominent features of the true dissociation geometry distribution can be restored by dividing the measured transverse Dalitz plot by the simulated transverse Dalitz plot for random dissociation geometries. This ‘‘weighting’’ procedure, which takes into account all details of the detection efficiency, at least allows one to clearly identify preferred or avoided breakup geometries. For a more quantitative analysis, one is bound to use the Monte Carlo image restoration technique [21], but to avoid the creation of artifacts this needs an experimental data set of much higher statistical significance and purity than available from the present experiment. The resulting Dalitz plots, obtained for D_2H^+ and H_2D^+ by using the weighting procedure after symmetrizing the data around $Q_1 = 0$, are displayed in the two lower panels of Fig. 2. Both distributions give evidence for an enhanced occurrence of certain linear dissociation geometries and reveal an unexpected isotope effect: In the H_2D^+ case [Fig. 2(c)] the data clearly show that the D atom prefers to be in the middle of the two hydrogen atoms, while no preferences

for the linear H-H-D and D-H-H geometries are observed. Similarly, for D_2H^+ [Fig. 2(d)] linear geometries with one of the two deuterons occurring between the hydrogen and the other deuteron seem to be preferred compared to the linear D-H-D configuration. The stability of this conclusion was checked by using different CM cuts (the 1σ CM cut is shown in the Fig. 2) to ensure that the observed features are not an artifact due to false identifications of the H and D fragments.

Enhancements of symmetric linear dissociation geometries were already found for H_3^+ and D_3^+ [21], but because the three constituents are indistinguishable the D_{3h} symmetry leads to a three-fold occupancy in the corresponding Dalitz plots; the small isotope effect indicated by the size of the enhancement when comparing H_3^+ and D_3^+ is likely due to the differences in the width of the initial wave function for these two isotopomers. On the other hand, for H_2D^+ and D_2H^+ the D_{3h} symmetry is broken and only the C_{2v} symmetry remains. Based on the Born-Oppenheimer approximation, the potential energy surfaces (PESs) of both the precursor ion and the neutral complex are identical to the symmetric (H_3^+ and D_3^+) case. On the other hand, the non-Born-

Oppenheimer Jahn-Teller coupling was found to play a crucial role in the theoretical treatment of the DR process for H_3^+ (Ref. [9]) and thus the nuclear species might indeed be suspected to produce asymmetries in the PES for H_2D^+ and D_2H^+ as compared to the symmetric isotopomers. Another possibility for the observed symmetry breaking might be related to kinematics: The force driving the breakup, which is initially equal for all fragments, causes a slower acceleration when acting on the D atom than on the H fragment, which breaks the fragment permutation symmetry in later phases of the dissociation process. It is felt that only detailed calculations of the three-dimensional wave packet propagation on the respective PES can shed more light on the preference for linear dissociation geometries and on the origin of the observed isotope effect.

This work has been funded in part by the German Israel Foundation for Scientific Research (GIF) under Contract No. I-707-55.7/2001, and by the European Community within the Research Training Network "Electron Transfer Reactions."

-
- [1] S. Lepp, *Nature (London)* **366**, 633 (1993).
 [2] E. Herbst and W. Klemperer, *Astrophys. J.* **185**, 505 (1973).
 [3] T. J. Millar, H. Roberts, A. J. Markwick, and S. B. Charnley, *Philos. Trans. R. Soc. London, Ser. A* **358**, 2535 (2000).
 [4] M. Larsson, *Philos. Trans. R. Soc. London, Ser. A* **358**, 2433 (2000).
 [5] B. J. McCall *et al.*, *Nature (London)* **422**, 500 (2003).
 [6] V. Poterya, J. Glosik, R. Plasil, M. Tichy, P. Kudrna, and A. Pysanenko, *Phys. Rev. Lett.* **88**, 044802 (2002).
 [7] V. Kokoouline, C. H. Greene, and B. D. Esry, *Nature (London)* **412**, 891 (2001).
 [8] V. Kokoouline and C. H. Greene, *Phys. Rev. Lett.* **90**, 133201 (2003).
 [9] V. Kokoouline and C. H. Greene, *Phys. Rev. A* **68**, 012703 (2003).
 [10] G. Sundström *et al.*, *Science* **263**, 785 (1994).
 [11] T. Tanabe, in *Dissociative Recombination: Theory, Experiment, and Applications*, edited by M. Larsson, J. Mitchell, and I. Schneider (World Scientific, Singapore, 2000), p. 170.
 [12] M. J. Jensen, H. B. Pedersen, C. P. Safvan, K. Seiersen, X. Urbain, and L. H. Andersen, *Phys. Rev. A* **63**, 052701 (2001).
 [13] H. Kreckel *et al.*, *Phys. Rev. A* **66**, 052509 (2001).
 [14] J. Glosik, R. Plasil, V. Poterya, P. Kudrna, M. Tichy, and A. Pysanenko, *J. Phys. B* **34**, L485 (2001).
 [15] R. Plasil *et al.*, *Int. J. Mass. Spectrom.* **218**, 105 (2002).
 [16] A. Le Padellec, M. Larsson, H. Danared, A. Larson, J. R. Peterson, S. Rosen, J. Semaniak, and C. Strömholm, *Phys. Scr.* **57**, 215 (1998).
 [17] M. Larsson, S. Lepp, A. Dalgarno, C. Stromholm, G. Sundstrom, V. Zengin, H. Danared, A. Källberg, M. af Ugglas, and S. Datz, *Astron. Astrophys.* **309**, L1 (1996).
 [18] S. Datz *et al.*, *Phys. Rev. A* **52**, 2901 (1995).
 [19] T. Tanabe *et al.*, in *Dissociative Recombination: Theory, Experiment, and Applications III*, edited by D. Zajfman, J. B. A. Mitchell, D. Schwalm, and B. R. Rowe (World Scientific, Singapore, 1996), p. 84.
 [20] L. Lammich *et al.*, *Phys. Rev. Lett.* **91**, 143201 (2003).
 [21] D. Strasser, L. Lammich, H. Kreckel, S. Krohn, M. Lange, A. Naaman, D. Schwalm, A. Wolf, and D. Zajfman, *Phys. Rev. A* **66**, 032719 (2002).
 [22] D. Strasser *et al.*, *Phys. Rev. Lett.* **86**, 779 (2001).
 [23] L. Lammich *et al.*, *Radiat. Phys. Chem.* **68**, 175 (2003).
 [24] A. Dalgarno, E. Herbst, S. Novick, and W. Klemperer, *Astrophys. J.* **183**, L131 (1973).
 [25] S. Miller, J. Tennyson, and B. T. Sutcliffe, *Mol. Phys.* **66**, 429 (1989).
 [26] R. H. Dalitz, *Philos. Mag.* **44**, 1068 (1953).